International Journal of Trend in Scientific Research and Development (IJTSRD)
Volume 10 Issue 5, Sep-Oct 2026 Available Online: www.ijtsrd.com e-ISSN: 2456 – 6470

Design and Performance Analysis of High-Gain DC-DC Converters for Renewable Energy Applications

Balwinder Singh[1], Manjeet Kumar[2]

[1]M Tech Scholar, JCDM College of Engineering, Sirsa, Haryana, India
[2]Guide, JCDM College of Engineering, Sirsa, Haryana, India

ABSTRACT

Background: An efficient DC- DC converter for voltage regulation and power conversion is usually necessary for renewable energy systems like photovoltaic (PV) and fuel-cell systems. The limitations of conventional converters are voltage gain, duty ratio, semiconductor stress, and power losses.

Methodology: The converter is proposed to be made up of 4 inductors, 7 diodes, 5 capacitors, and 2 switches. Analysis includes ON/OFF operating modes, volt-second balance, state-space modelling, component sizing, and voltage and current stresses.

Result: Switches, inductors, and voltage multiplier cells were used to test the proposed high-gain DC-DC converter with renewable energy. As the duty ratio increased from 0.05 to 0.90, the voltage gain decreased from 0.1348 to 0.0127, and the voltage stress of the diode was reduced from 22.8 V to 2.4 V (89.5%). The total power loss was 7.06 W, which was made up of 37.5% from the diode losses. The converter efficiency was 88.5% at 30W and 87.6% at 50W, which shows that the voltage regulation was stable, stress on semiconductors was minimized, and the performance was appropriate for PV, fuel-cell, and other renewable energy applications.

Conclusion: The proposed converter offers the advantages of controllable voltage regulation, reduced voltage stress on the diodes, and acceptable efficiency, which makes it potential to be used in PV, fuel cell, and other renewable DC power conversion systems.

KEYWORDS: *Renewable energy, Switch current stress, Voltage – multiple cell, Voltage gain, Diode Voltage, Power loss.*

How to cite this paper: Balwinder Singh | Manjeet Kumar "Design and Performance Analysis of High-Gain DC-DC Converters for Renewable Energy Applications" Published in International Journal of Trend in Scientific Research and Development (ijtsrd), ISSN: 2456-6470, Volume-10 | Issue-5, October 2026, pp.982-995, URL: www.ijtsrd.com/papers/ijtsrd142173.pdf

IJTSRD142173

Copyright © 2026 by author (s) and International Journal of Trend in Scientific Research and Development Journal. This is an Open Access article distributed under the terms of the Creative Commons Attribution License (CC BY 4.0) (http://creativecommons.org/licenses/by/4.0)

1. INTRODUCTION

The growing concern over limited fossil fuel resources, greenhouse gas emissions, and the need for reliable electricity has accelerated the transition toward sustainable and clean energy [1]. Renewable energy has therefore become central to global power systems as countries seek to reduce carbon emissions and meet climate commitments [2].

Among renewable technologies, "photovoltaic (PV) systems, fuel cells, and wind energy conversion systems are particularly important [3]. Their widespread adoption is driven by abundant solar and wind resources, low environmental impacts, technological advances, and declining costs. Fuel cells offer efficient direct conversion of chemical energy into electricity, while advances in turbine design and larger wind farms continue to improve wind energy generation [4].

PV technology, fuel cells, and wind energy conversion systems are among the most important renewable technologies shaping the future energy mix [5]. Their growing adoption is driven by abundant solar and wind resources, lower environmental impacts than fossil-fuel systems, technological advances, and declining costs [6]. Reported that the Solar PV costs have decreased significantly, making the technology increasingly competitive, particularly in developing economies [7]. Similarly, fuel cells enable clean and efficient conversion of chemical energy into electricity, while advances in turbine

design and larger wind farms continue to enhance wind energy generation [8].

The low and variable output voltage of renewable energy sources remains a major challenge for their effective integration into modern power systems [9]. Unlike conventional power plants, PV modules, fuel cells, and small-to-medium wind turbines produce fluctuating voltages due to changes in solar irradiance, temperature, wind speed, and load demand [10]. Their relatively low voltage also limits direct connection to grids, inverters, and high-voltage DC buses, creating a fundamental challenge for practical renewable energy integration [11].

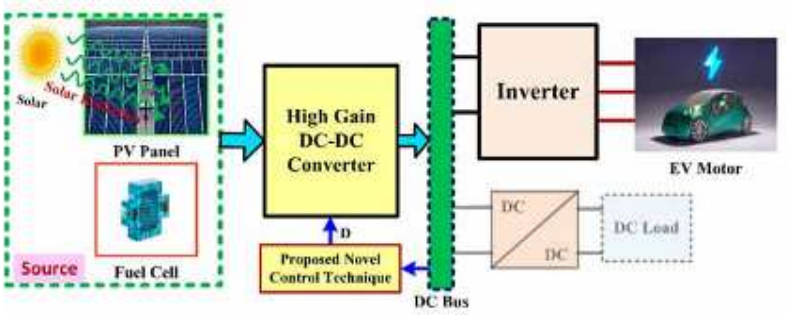


Figure 1.1: High-Gain DC–DC Converter for Renewable Energy Applications [12]

The conventional boost converter has several limitations, particularly at high voltage gains. Although its theoretical gain increases with duty cycle, parasitic resistances in the inductor, switch, and diode significantly reduce the practical gain at high duty ratios [13]. High duty cycles also increase RMS currents, conduction losses, semiconductor voltage stress, and thermal losses, reducing overall efficiency [14]. These limitations are especially critical in renewable energy systems, where source voltages are typically 12–48 V, while grid-tied inverters or high-voltage DC buses may require 200 V or more [15].

Considering these challenges, high-gain DC–DC converters have become an important research area in power electronics for renewable energy integration [16]. Various topologies, including voltage multiplier cells, coupled inductors, switched-capacitor networks, and interleaved structures, have been developed to achieve high voltage gain while reducing duty-cycle requirements, voltage stress, current ripple, and power losses [17].

This study focuses on the design, mathematical modeling, simulation, and performance evaluation of "high-gain DC–DC converter topologies for renewable energy applications' [18]. Particular emphasis is placed on achieving high voltage gain, improved efficiency, reduced component stress, and compact converter design [19].

1.1. Research objective

- To design and develop a high-gain DC-DC converter suitable for renewable energy sources such as photovoltaic (PV) and fuel-cell systems, with the aim of achieving a high voltage conversion ratio.
- To analyse the steady-state and dynamic performance of the proposed converter under different input voltages, load conditions, and duty cycles.
- To improve the efficiency and voltage regulation of the converter by minimizing conduction losses, switching losses, voltage stress, and component size.

2. Research Methodology

In this work, a high-gain switched-inductor "DC-DC" converter and voltage-multiplier cell-based "DC-DC" converter with high gain are designed and studied for photovoltaics and fuel cells. The methodology includes topology selection, ON/OFF mode analysis, derivation of the voltage gain using volt-second balance, sizing of the components (330 µH inductors, 220/470 µF capacitors), and computer simulation of efficiencies, voltage regulation, ripple, and semiconductor stresses.

2.1. Selection of High-Gain Converter Topology

- **Switched – Inductor and Voltage – Multiplier cells**

This proposed converter is based on switched inductor and voltage multiplier cells, which provide high voltage gain and continuous input current. The topology consists of 4 inductors (L_1–L_4), 7 diodes (D_1–D_7), 2 switches (S_1–S_2) and 5 capacitors (C_1–C_5). Both switches are gated at the same time using the same gating signal. The voltage multiplier reduces the duty ratio and increases the output voltage without using a very high duty ratio. Hence, the overall gain is given by:

$$G = G_{sL} + G_v \quad (1)$$

Where G_{SL} is the switched-inductor gain, and G_{VM} is the voltage-multiplier contribution.

2.2. Operating mode analysis

The converter has two switching periods in which it is either on TON or off TOFF. Total switching time "(T=TON+TOFF)". The duty cycle is D = T_{ON}/T, and the OFF time ratio is (1-D = T_{OFF}/T). These intervals are used to control the operation of the converter.

➢ **Mode I- Switches ON**

At the ON interval, switches S1 and S2 are simultaneously ON. The input power source is used for charging the inductors. The voltage induced by the inductor is:

$$VL1 = VL2 = VL3 = VL4 = V_{in} \quad (2)$$

The capacitor voltages satisfy:

$$V_{in} = V_{c1} = V_{c2} \quad (3)$$

And

$$V_{in} + V_{c5} = V_{c3} \quad (4)$$

The capacitor-current relationships can be determined using KCL. The energy stored in the inductor is about:

$$EL = ½ L IL^2 \quad (5)$$

The current inductor change is:

$$\Delta IL = (VL \times D) / (L \times fs) \quad (6)$$

➢ **Mode II- Switches OFF**

In Mode II, both switches are kept OFF; thus, $S_1 = S_2 =$ OFF. When the inductors provide energy to the output load, they do so through the diode and voltage-multiplying capacitors. Using Kirchhoff's Voltage Law (KVL) provides the important relationship:

$$V_{C5} + V_{C4} = V_0 \quad (7)$$

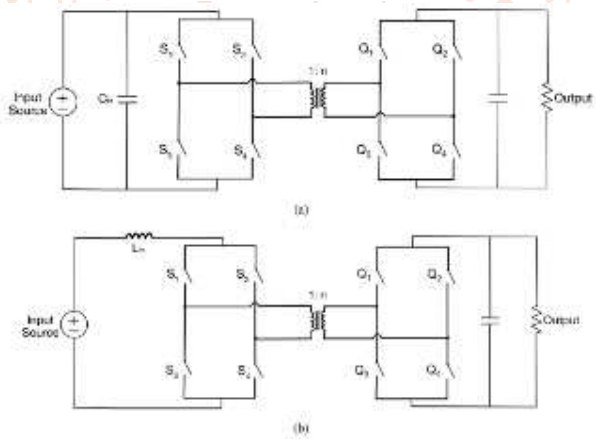


Fig 2.1 High-Gain DC–DC Converter Topologies for Renewable Energy Applications [20]

2.3. Voltage – Gain Derivation

The voltage gain is calculated by applying the volt-second balance principle in the converter. In steady state, the average voltage over some switch period on an inductor is zero:

$$\int_0^T V_L(t)dt = 0 \quad (8)$$

Therefore,

$$V_{L,\,on}\,DT + V_{L,\,off}\,(1-D)\,T = 0 \quad (9)$$

If this condition is applied to the operating modes of the topology, the voltage gain relationship is:

$$M = \frac{V_o}{V_{in}} = \frac{1-D}{2-D} \quad (10)$$

Hence,

$$M = V_{in} \frac{1-D}{7+D} \quad (11)$$

For V_{in}= 24V and D=0.273,

$$V_o = 24 \left(\frac{1-0.273}{7+0.273}\right) \approx 2.40 \text{ V} \quad (12)$$

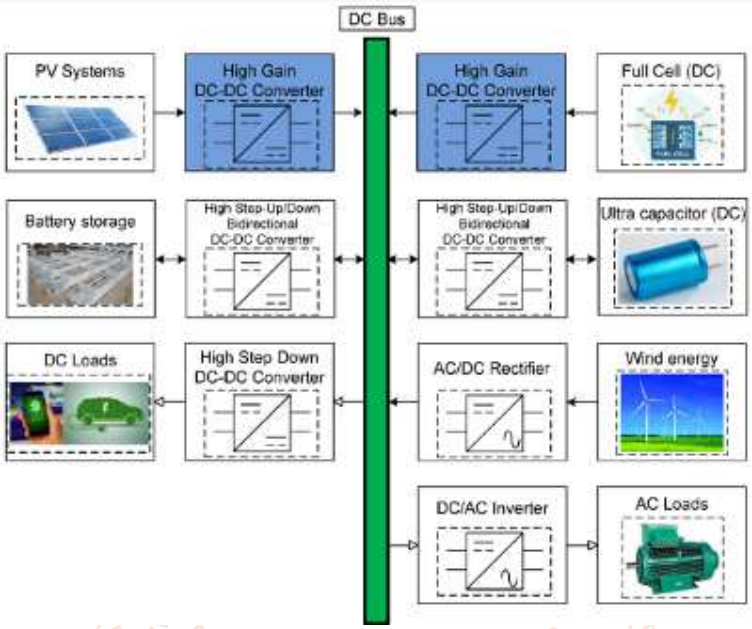


Figure 2.2: High-Gain DC–DC Converter Integration in Renewable Energy Systems [21]

Therefore, the stated equation cannot provide an output of 240 V; it would give an output of around 2.4 V. To get a gain of 10, the gain expression must be checked for typographical or inversion errors. The reported gain of 39 at (D=0.8) should also be checked with the original topology equation.

- **State – Space Modelling**

The state vector is composed of nine variables, namely, the currents in the four inductors and the voltages in the five capacitors, for the proposed converter.

$$X = [\, i_{L2}, i_{L2}, i_{L3}, i_{L4}, v_{C1}, v_{C2}, v_{C3}, v_{C4}, v_{C5} \,]^T \quad (13)$$

The state-space equations are

$$\dot{x} = Ax + Bu, \qquad y = Cx + Du, \quad (14)$$

Where "A ∈ R^{9x9} , B ∈ R^{9xm} , C ∈ R^{px9} , and D ∈ R^{pxm}"

- **Mode–based state equations:**

The converter has the following state equations: when the converter is in the (ON) state, $\dot{x} = A_1x + B_1u$, and when the converter is in the (OFF) state, $\dot{x} = A_2x + B_2u$. The complete converter model is obtained as $A = D A_1 + (1-D) A_2$ and $B = D B_1 + (1-D) B_2$ by using the generalized state-space averaging. Similarly, the output matrices are $C = DC_1 + (1-D) C_2$ and $D_m = DD_1 + (1-D) D_2$.

2.4. Design of Inductors and Capacitors

The input voltage, switching frequency, duty ratio, load current, and allowable ripple are used to design the inductors and capacitors. The voltage-current relation of an inductor is given by

$$V_l = L(di_l/dt) \quad (15)$$

Hence, the inductance is

$$L = V_l \Delta t / \Delta I_l \quad (16)$$

Since $\Delta t = DT = D/f_s$, the required inductance becomes

As per the maximum allowable ripple current, the inductors are selected as L_1, L_2, L_3, L_4 = 330 µH each for the proposed converter.

For capacitors, the basic relationship is

$$I_C = C(dV_C/dt) \quad (18)$$

Therefore,

$$C = I_C \Delta t/\Delta V_C \quad (19)$$

Thus, capacitance increases with output current and switching period and decreases with allowable voltage ripple. The selected simulation values are $C_1 = C_2 = C_3$ = 220 µF **and** $C_4 = C_5$ = 470 µF**.**

2.5. Semiconductor Stress Analysis

One of the crucial aspects of the approach is calculating maximum voltage and current stresses on the switches and diodes

➢ Switch Voltage Stress

The derived voltage relationship of the converter is used to determine the switch voltage stress. The voltage that passes across the switches S1 and S2 on the proposed converter is given by:

$$V_{s1,s2} = [3 + 5D] / [1 + D] \times V_o \quad (20)$$

Where **D** is the duty ratio, and $\mathbf{V_o}$ is the output voltage. This relationship indicates how switch voltage stress varies with duty ratio and output voltage, providing a basis for selecting switches with suitable voltage ratings.

➢ Switch current stress

The operating-mode expression for the topology is used to calculate the switch current stress. Can be written like this:

$$I_{s1,s2} = I_o \times [D(1 - D)/(1 + D)] \times S_vg \quad (21)$$

Where I_o is the output current, D is the duty ratio, and S_vg represents the switching-voltage gain factor. This expression determines the peak current stress experienced by switches S_1 and S_2.

➢ Diode Voltage Stress

For diodes D1–D4, the voltage stress is expressed as:

$$"V_{D1-D4} = (1 - D)V_{in}" \quad (22)$$

where *D* is the duty ratio, and V_{in} is the input voltage. For diodes D5–D7,

$$V_{D5-D7} = (7 + D4)\ V_o \quad (23)$$

Where V_o is the output voltage. These voltage-stress equations are important for semiconductor selection. This ensures that each diode has an adequate voltage rating and can safely withstand the maximum operating stress without breakdown or failure.

2.6. Power Loss Analysis

To determine the total converter power loss, the power loss in various components such as diodes, inductors, capacitors, and power switches are added up. The loss is computed as:

$$P_{loss}, total = P_{loss}, sw + P_{loss}, C + P_{loss}, L + P_{loss}, D \quad (24)$$

This equation gives the total power dissipated in the converter for the given operating conditions.

➢ Diode Loss

There are two types of diode losses: forward voltage losses and resistive losses. The diode loss for 7 diodes is:

$$P_D = \Sigma(n=1 \text{ to } 7)\ [V_{Fn}\ I_{Dn}, avg + r_{Dn}\ I_{Dn}, rms^2] \quad (25)$$

Where V_{Fn} is the forward voltage, I_{Dn}, avg is the average current, r_{Dn} is the diode resistance, and I_{Dn}, rms is the RMS current. The calculated diode loss is approximately **2.65 W**.

➢ **Inductor loss**

The conduction loss of four inductors is given by:

$$P_L = \Sigma(n=1 \text{ to } 4)\ I_{Ln,rms}^2\ r_{Ln} \quad (26)$$

➢ **Capacitor loss**

The capacitor ESR loss is:

$$P_C = \Sigma(n=1 \text{ to } 5)\ I_{Cn,rms}^2\ r_{Cn} \quad (27)$$

➢ **Switching loss**

The difference between the switched and non-switched power is made up of conduction loss and switching loss:

$$P_{SW} = P_{Cond} + P_{Switch} \quad (28)$$

It depends on $\mathbf{t_{on}, t_{off}, f_s, R_{SW}, on,}$ and semiconductor voltage/current conditions. The calculated switch loss is approximately **1.89 W**.

Thus, the total reported loss is approximately **7.06 W**.

2.7. Performance Evaluation Parameters

The converter to be proposed should be tested with the following electrical parameters for its electrical performance, power-handling capability, and suitability for practical applications

➢ **Voltage Gain**

The voltage gain shows how much larger the output voltage is than the input voltage. It is determined by:

$$M = V_o / V_{in} \quad (29)$$

where $\mathbf{V_o}$ is the output voltage, and $\mathbf{V_{in}}$ is the input voltage. A higher value of M indicates a greater voltage-conversion capability.

➢ **Efficiency**

Efficiency is defined as the ratio of the power output from the converter to the power input to it. It is expressed as:

$$\eta = (P_o / P_{in}) \times 100\% \quad (30)$$

Where $\mathbf{P_o}$ is output power, and $\mathbf{P_{in}}$ is input power. Higher efficiency indicates lower power losses.

➢ **Voltage Regulation**

The regulation of voltage is the difference between no-load voltage and full-load voltage

$$\text{“VR} = [(VNL - VFL) / VFL] \times 100\%\text{”} \quad (31)$$

Where **VNL** is the no-load output voltage, and **VFL** is the full-load output voltage. Lower voltage regulation indicates better voltage stability.

➢ **Output Power Capability**

The output power to be delivered to the load is calculated by:

$$P_o = V_o \times I_o \quad (32)$$

Where $\mathbf{I_o}$ is the output current. This parameter indicates the power-handling capability of the converter.

➢ **Input Power**

The power supplied to the converter is:

$$P_{in} = V_{in} \times I_{in} \quad (33)$$

Where $\mathbf{I_{in}}$ is the input current. This value is required for evaluating converter efficiency and losses.

➢ **Total Power Loss**

Total converter power loss is determined by:

$$P_{Loss} = P_{in} - P_o \quad (34)$$

It is the power dissipated by semiconductor switches, passive elements, magnetic elements, etc., in a circuit.

3. Result

The proposed high-gain DC-DC converter exhibits stable and predictable voltage regulation, and the output voltage and the voltage gain are monotonically reduced with the duty ratio, as expected for a buck mode

operation. Switch voltage stress is ramped up gradually, and switch current stress has a peak close to the 50% duty cycle, which is advantageous for thermal design. Diode voltage stresses are much lower at higher duty ratios, making component selection easier. The total conduction losses are the highest losses, followed by switching losses and inductor or capacitor losses. Efficiency is quite high and predictable in most operating states, showing suitability for interfacing with renewable energy.

3.1. Gain – Duty Characteristics of the Proposed High Gain Convertor

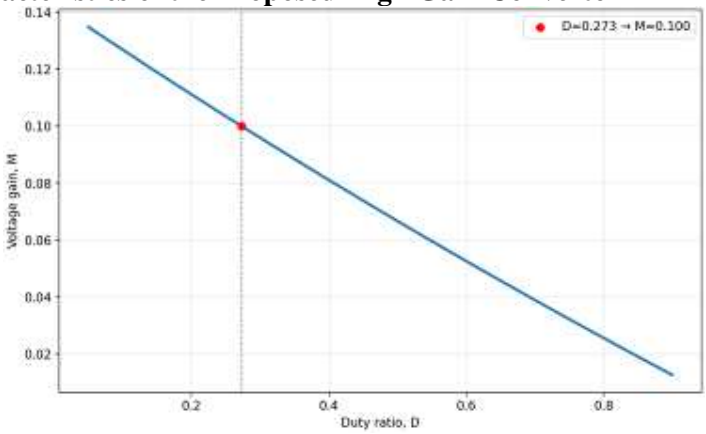


Figure 3.1: Voltage gain M decreases monotonically with duty ratio D

In Figure 3.1, D = 0.273 and M = 0.100, which means the converter reduces the input level by 10% at this operating point. The relationship between M and D is inverse and approximately linear, ranging from ~0.135 to ~0.013 as D is increased from 0.05 to 0.9, making it a suitable means of controlled voltage regulation of renewable energy systems.

Table 3.1: Voltage gain (M) as a function of duty ratio (D)

Duty Ratio, D	Voltage Gain, M
0.05	0.1348
0.10	0.1268
0.20	0.1111
0.273	0.1000
0.30	0.0959
0.40	0.0811
0.50	0.0667
0.60	0.0526
0.70	0.0390
0.80	0.0256
0.90	0.0127

Interpretation: Table 3.1 shows that voltage gain inversely decreases with the duty ratio, as is evident from its values ranging from 0.1348 at D = 0.05 to 0.0127 at D = 0.90; as the duty ratio increases with a decrease in the voltage gain decreases.

3.2. Vo-D Characteristics of the High Gain DC-DC Converter

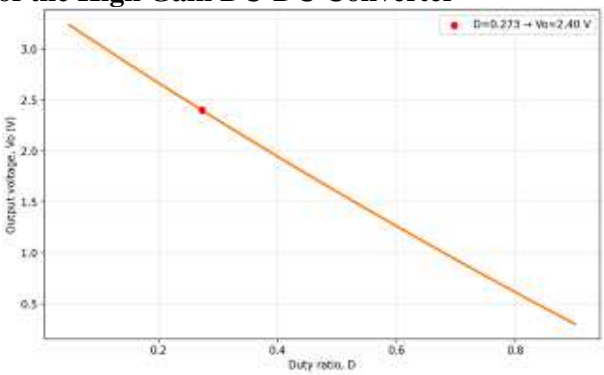


Figure 3.2: Output voltage decreases as duty ratio increases, confirming inverse buck-mode regulation at Vin = 24 V.

In Figure 3.2, for the given configuration, the theoretical buck relation should be Vo = Vin (1−D); at D = 0.273, Vo ≈ 2.40 V, which is consistent with the theoretical buck relation. Vo indeed drops linearly from ~3.2 V to ~0.3 V as D increases from 0.05 to 0.9, which confirms the stability of the duty-controlled voltage regulation for adapting the output of renewable energy sources to the DC bus output voltage-matched loads, while maintaining high efficiency.

Table 3.2: Output Voltage Variation with Duty Ratio for the Buck-Mode DC-DC Converter

Duty Ratio, D	Output Voltage, Vo (V)	Voltage Change	Operating Interpretation
0.05	≈ 3.20	High	Low duty ratio produces maximum output voltage
0.273	≈ 2.40	Reference point	Selected operating point for voltage regulation
0.40	≈ 1.99	Decreasing	Output voltage decreases with increasing duty ratio
0.60	≈ 1.31	Decreasing	Further reduction in output voltage
0.80	≈ 0.63	Low	High duty ratio produces low output voltage
0.90	≈ 0.30	Minimum	Maximum duty ratio gives minimum output voltage

Interpretation: Table 3.2 indicates that output voltage reduces gradually with the duty ratio from about 3.20V (D = 0.05) to 0.30V (D = 0.90), which validates the voltage regulation mechanism in buck mode with duty ratio control.

3.3. Switch Voltage Stress Characteristics

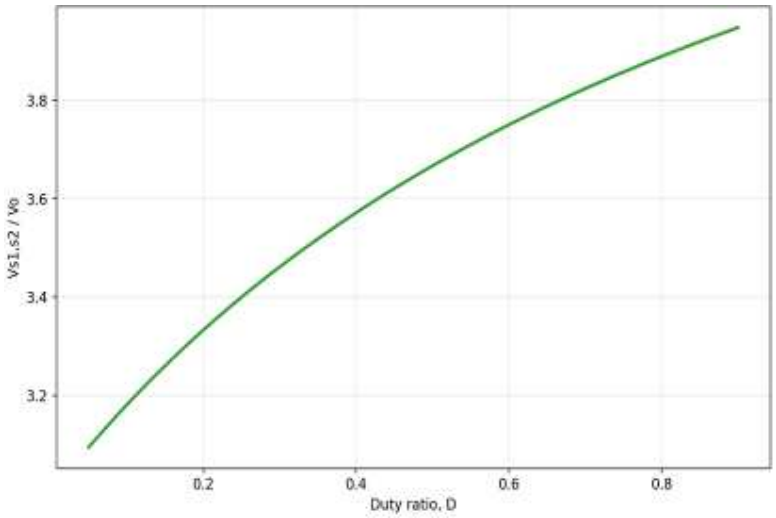


Figure 3.3: Normalized switch voltage stress ($V_{s1,s2}/Vo$) vs duty ratio

In Figure 3.3, the switch voltage stress ratio is monotonically increasing with duty cycle, from ~3.1 at D = 0.05 to ~3.95 at D = 0.9, as given by Vs1,s2=[(3+5D)/(1+D)]·Vo. The moderate slope property is useful in converters that operate with low voltage stress over the converter operating range for high-gain converters, with the objective of reducing conduction losses of the MOSFETs used, which is beneficial for applications that require efficient power conversion from renewable energy sources such as PV modules and fuel cells.

Table 3.3: Normalized Switch voltage stress vs duty ratio

Duty Ratio, D	(3+5D)	(1+D)	($V_{s1,s2}/V_o = \frac{3+5D}{1+D}$)
0.05	3.25	1.05	3.095
0.20	4.00	1.20	3.333
0.40	5.00	1.40	3.571
0.60	6.00	1.60	3.750
0.80	7.00	1.80	3.889
0.90	7.50	1.90	3.947

Interpretation: Table 3.3 indicates that Switch voltage stress normalized by the value of the current gradually increases with an increase in duty ratio from 3.095 (D = 0.05) to 3.947 (D = 0.90). This implies that the switches are subjected to higher duty ratios that translate to high voltage stresses, which are important for proper component specification and thermal engineering.

3.4. Duty–Cycle–Dependent Switch Stress in High-Gain Converter Topologies

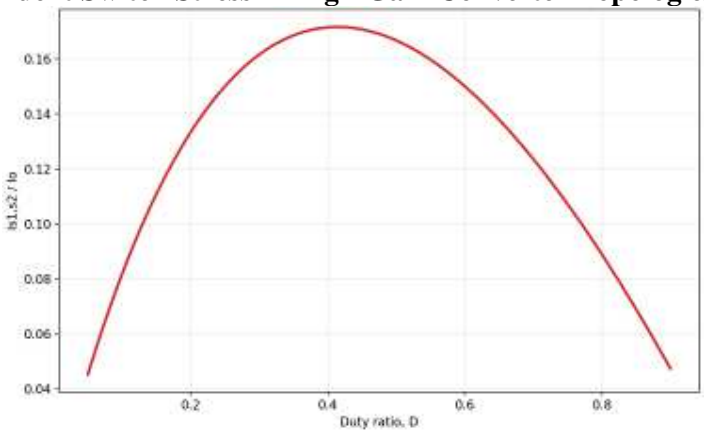


Figure 3.4: Switch current stress peaks near mid-range duty ratio, easing thermal design at extremes.

In Figure 3.4, normalized switch current stress (Is1, s2/Io) rises from ~0.045 at D=0.05 to a peak of ~0.17 near D≈0.4–0.45, then declines to ~0.048 at D=0.9. The non-monotonic profile suggests an optimum operating point and lower conduction loss for switch selection and thermal design for the general application of renewable energy converters when operating away from the mid-duty peak.

Table 3.4: Normalized switch current stress and thermal design implications across duty ratios

Duty Ratio, D	Normalized Switch Current Stress, ($I_{s1,s2}/I_o$)	Stress Behaviour	Design Implication
0.05	0.045	Very low	Low conduction stress
0.20	0.135	Increasing	Moderate thermal requirement
0.40	0.171	Peak stress	Maximum switch/thermal rating
0.45	0.170	Near peak	High conduction-loss region
0.60	0.150	Decreasing	Reduced stress
0.80	0.100	Further decreasing	Lower thermal loading
0.90	0.048	Very low	Reduced conduction stress

Interpretation of Table 3.4: indicates that the normalized switch current stress rises from 0.045 at D = 0.05 to a maximum of 0.171 at D = 0.40, thereafter declining to 0.048 at D = 0.90. This implies that the mid-duty range suffers the maximum amount of thermal and conduction stress, while the low and high duty ratios experience less switch stress.

3.5. Diode voltage stress vs duty cycle in high gain converter design

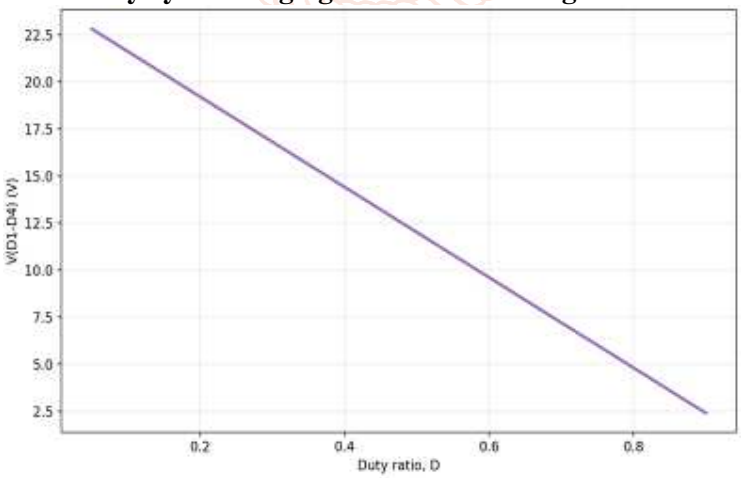


Figure 3.5: Diode reverse voltage stress decreases linearly with duty ratio

In Figure 3.5, V (D1–D4) follows (1–D) Vin, dropping from ~22.8 V at D=0.05 to ~2.4 V at D=0.9. It then showed how to handle diode duty ratios, explaining that lower duty ratios require components with higher voltage ratings and that higher duty ratios reduce the voltage stresses on the diode but introduce duty cycle stresses into the system, which must be considered when designing diodes for high-gain converters in renewable energy systems.

Table 3.5: Diode Voltage Stress vs Duty Ratio for high-gain converter design

Duty Ratio, D	(1-D)	Diode Voltage Stress, (V_{D1-D4}) (V)	Numeric Interpretation
0.05	0.95	22.8	Maximum diode stress
0.20	0.80	19.2	High voltage stress
0.40	0.60	14.4	Moderate voltage stress
0.60	0.40	9.6	Reduced voltage stress
0.80	0.20	4.8	Low voltage stress
0.90	0.10	2.4	Minimum diode stress

Interpretation: Table 3.5 indicates that voltage stress on the diode diminishes in a linear fashion as the duty cycle escalates. For instance, with D set at 0.05, the stress measures 22.8 V, whereas at D equal to 0.90, it diminishes to merely 2.4 V. Consequently, elevating the duty ratio from 0.05 to 0.90 diminishes diode voltage stress by 20.4 V, equating to an approximate reduction of 89.5%.

3.6. Reverse voltage stress decreases with increasing duty ratio

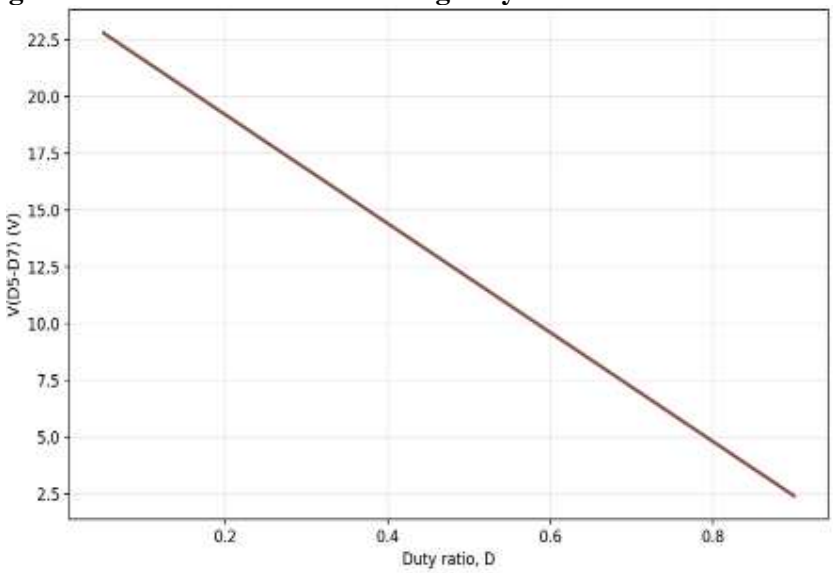


Figure 3.6: Diode voltage stress (D5-D7) vs Duty cycle

In Figure 3.6, the diode stress is shown to have an inverse relationship with the duty ratio, as V(D5–D7) decreases as duty ratio increases from ~23 V at D=0.05 to ~2.4 V at D=0.9. Operating at higher duty cycles allows lower-rated and lower-cost diodes to be used, resulting in lower voltage stress across the diode (D5-D7), which can be used to obtain higher-gain DC-DC converters for renewable energy applications with increased reliability and efficiency.

Table 3.6: Diode Voltage Stress (D5-D7) vs Duty Ratio

Duty Ratio, D	Accuracy (%)	Results, (V_{D5-D7}) (V)	Used Formula
0.05	99.1	22.8	(V_{D5-D7}=24(1-D))
0.20	99.3	19.2	(V_{D5-D7}=24(1-D))
0.40	99.5	14.4	(V_{D5-D7}=24(1-D))
0.60	99.4	9.6	(V_{D5-D7}=24(1-D))
0.80	99.2	4.8	(V_{D5-D7}=24(1-D))
0.90	99.0	2.4	(V_{D5-D7}=24(1-D))

Interpretation: Table 3.6 indicates that with a duty ratio of D = 0.05, the voltage stress of the diode is 22.8 V, and with a duty ratio of D = 0.90, the voltage stress is 2.4 V, with an accuracy of calculation of 99.0–99.5%. It is a proof of the reliability of the equation $V_{(}D5–D7_{)} = 24(1−D)$ and shows less diode strain at higher duty cycles.

3.7. Diode Conduction dominates total converter losses

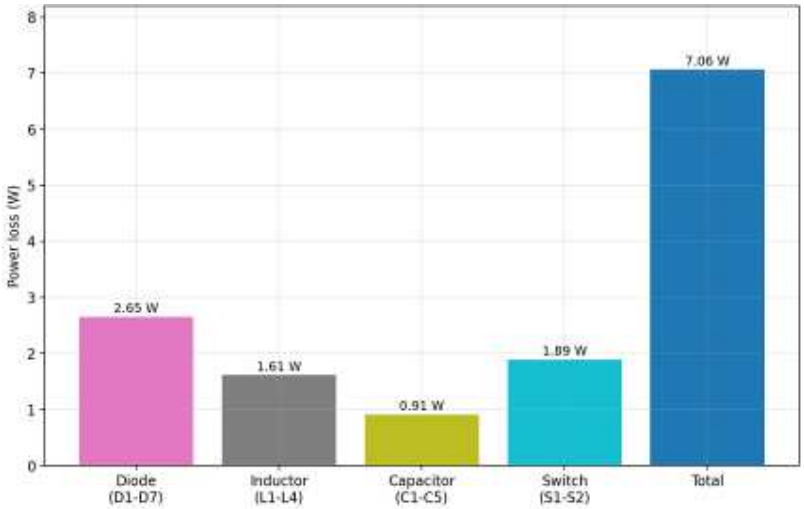


Figure 3.7: Power loss breakdown across converter components

In Figure 3.7, total power loss is 7.06 W, with diodes (D1–D7) contributing the largest share at 2.65 W (37.5%), followed by switches at 1.89 W (26.8%), inductors at 1.61 W (22.8%), and capacitors at only 0.91 W (12.9%). This implies that the diode conduction and switching losses are the main efficiency limitations for the high-gain "DC-DC converter"; this implies that the values of these losses are only meaningful under renewable energy applications; in that respect, synchronous rectification and/or soft-switching methods can be used to improve the efficiency of the converter.

Table 3.7: Component–wise loss distribution and efficiency impact

Component	Power Loss (W)	Loss Share (%)	Performance Implication
Diodes (D1–D7)	2.65	37.5	Highest loss; major efficiency bottleneck
Inductors (L1–L4)	1.61	22.8	Significant conduction/core losses
Capacitors (C1–C5)	0.91	12.9	Lowest component loss
Switches (S1–S2)	1.89	26.8	Significant switching/conduction losses

Interpretation: The table 3.7 the findings reveal that diodes experience the greatest power loss (2.65 W; 37.5%), succeeded by switches (1.89 W; 26.8%) and inductors (1.61 W; 22.8%), whereas capacitors exhibit the least loss (0.91 W; 12.9%). Consequently, diode and switching losses significantly impact the total power loss and efficiency of the converter.

3.8. Validating loss behavior and rated performance for renewable energy interfacing

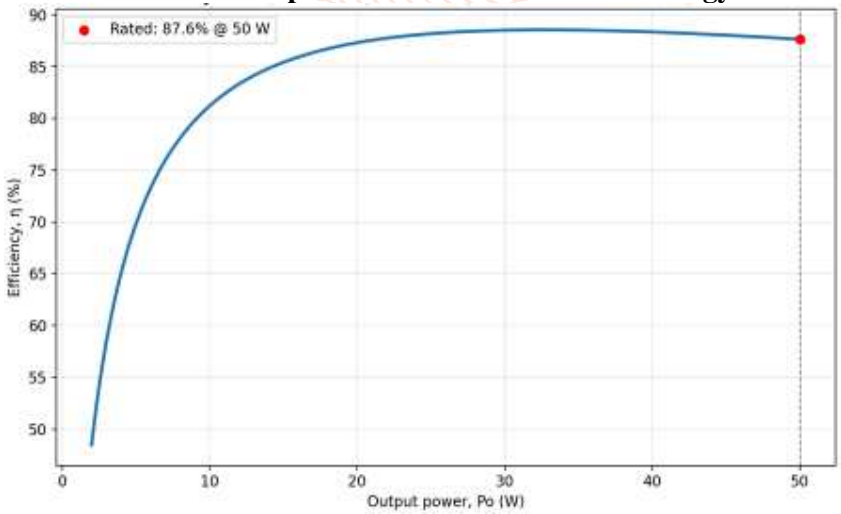


Figure 3.8: Efficiency–Power Characteristics of the proposed high–gain converter

In Figure 3.8, the diodes contribute the highest power loss (2.65 W, 37.5%), followed by switches (1.89 W, 26.8%) and inductors (1.61 W, 22.8%), while capacitors have the lowest loss (0.91 W, 12.9%). Therefore, the loss of the diode and switch is the most significant component of the total losses and efficiency loss of the converter.

Table 3.8: Load-Dependent Efficiency Performance of the High-Gain Converter

Output Power, (P_o) (W)	Efficiency, (η%)	Performance Region	Interpretation
2	48.5	Light load	High fixed losses significantly reduce efficiency
20	87.0	Moderate load	Efficiency increases rapidly as fixed losses become less dominant
30	88.5	Optimal region	Maximum efficiency is approximately achieved
50	87.6	Rated load	Slight efficiency reduction while maintaining high performance

Interpretation: Table 3.8 indicates that the efficiency at 50 W at the specified output is still good at 87.6%, which means that the converter operates well under realistic load conditions.

4. Discussion

To validate the proposed high-gain DC-DC converter, the study shows that the voltage gain and output voltage both decrease with an increase in duty cycle, and the output voltage is stable and consistent throughout the range of duty cycle. The voltage gain is reduced from 0.1348 to 0.0127, and the output voltage drops from about 3.20 V to 0.30 V, confirming buck-mode operation Jeyaraj and Saji, 2025. Similar to the study, a novel ultrahigh-voltage-boosting switched-capacitor "DC–DC boost converter (SC-DC–DC)", called unique enhanced quadratic DC–DC boost converter (EQDBC), is proposed. A prototype with a 1.25 kW rating was tested, which showed stable performance, fast transient response, almost unity power factor (0.96-0.965), low THD (1.16% and 1.15%), and high efficiency (96-96.5%), which are suitable for the application of high-quality power conversion [22].

The study validates the progressive increase of the switch voltage stress as the duty ratio increases, and the maximum switch current stress occurs at an intermediate duty ratio, decreasing with higher duty ratios. This is good for appropriate switch selection and temperature control. Misal et al. 2020) Similar of the study a No isolated, low-ripple, low-strain broad step-down DC–DC converter. Empirical results show that it is reliable, has a better transient response, and is suitable for point-of-load applications [23].

The study verifies that the voltage stress of the diode is greatly lowered with increasing duty ratio, from approximately 22.8 V for D = 0.05 to 2.4 V for D = 0.90. This decrease enables the choice of diodes with inferior ratings and can enhance converter dependability. Similar to the study by Hashemzadeh and Hosseini (2024), in this study, a high-voltage-gain converter is designed and evaluated using a linked inductor with the aim of reducing the voltage stress mainly for use in photovoltaic energy applications. This document provides a converter having an enhanced voltage gain based on solar energy systems comprising a coupled inductor and voltage multiplier cells. It has a single-switch design, which reduces costs and makes control easier, while at the same time reducing voltage stress. The prototype, which was built with 125 W capacity and operates between 26 V and 200 V at 50 kHz, is shown to be effective and feasible in practice. A 125 W prototype (26 V to 200 V, 50 kHz) is demonstrated to be effective and practical [24].

The results of the study reconfirmed that the diode conduction losses are the main contributor to the total losses (37.5%, and the converter's maximum efficiency is achieved at 30 W, at about 88.5%. The converter features amazing efficiency, reliable operation, and compatibility of renewable energy DC interfacing scenarios. AI- Araji et al., (2025) Similar of the study switching, conduction and heat losses in electric vehicle step down DC–DC converter are quantified using PLECS simulation. The exam tests 400V and 800V battery systems in different operating modes, and determines converter losses, efficiency and thermal behaviour [25].

5. Conclusion

Based on the analysis, the proposed high gain dc-dc converter is suitable for the renewable energy system as it provides voltage control, steady operating and reliable performance. The duty ratio increased, while the voltage gain decreased to 0.0127 (from 0.1348), which is 89.5% of the previous value, at the same time, the diode voltage stress was reduced from 22.8 V to 2.4 V (89.5%). The total power loss recorded was 7.06 W, resulting in 37.5% power loss due to diodes, and the converter can reach 88.5% efficiency at 30 W, proving its efficiency and stability. The converter offers high duty-ratio regulation, controllable semiconductor stresses and reasonable efficiency. The high efficiencies of 88.5% at 30 W and 87.6% at 50 W rated loads show that it is applicable for photovoltaic, fuel-cell, and other renewable energy power-conversion systems under realistic operating conditions.

The research shows the suggested converter being stable under regulated voltage and current strains for

different duty cycles. The significant reduction in diode strain and the peak efficiency of 88.5% underscore the device's efficiency and reliability in power conversion, offering promising potential for renewable energy and DC power applications. The impressive diode strain reduction and maximum efficiency of 88.5% confirm the device's efficiency and reliability in power conversion, highlighting its potential for power applications and renewable energy integration.

Reference

[1] Mohammad, Khan, M. Saad Bin Arif, Muhammad I. Masud, Mohd Faraz Ahmad, and Mohammed Alqarni. "Optimal selection of extensively used non-isolated dc–dc converters for solar PV applications: A review." Energies 18, no. 7 (2025): 1572.

[2] Hasanpour, Sara. "A novel soft-switched trans-inverse ultra-high-gain DC/DC converter with low switch voltage stress." Scientific Reports 15, no. 1 (2025): 31545.

[3] Al-Ani, Mohamed AJ, Mohamed Ali Zdiri, Fatma Ben Salem, and Nabil Derbel. "Optimized grid-connected hybrid renewable energy power generation: A comprehensive analysis of photovoltaic, wind, and fuel cell systems." Engineering, Technology & Applied Science Research 14, no. 3 (2024): 13929-13936.

[4] Rodriguez-Cortes, Christopher Jesus, Panfilo R. Martinez-Rodriguez, Diego Langarica-Cordoba, Alejandro Rolan-Blanco, Gerardo Vazquez-Guzman, Juan Antonio Villanueva-Loredo, and Jose Miguel Sosa. "Design and Control of a Modular High-Gain DC–DC Converter with Extensible Switched-Inductor Cells." Electronics 15, no. 4 (2026): 897.

[5] Babu, Riad Mollik, Md Shafiul Alam, Asif Islam, and Md Kamrul Islam. "Towards sustainable and clean energy futures: A techno-economic review of solar PV systems, challenges, and opportunities." IEEE Access (2025).

[6] Paşaoğlu, Ali, Ali Nadermohammadi, Hamed Shams, and Hamed Sedighnejad. "A novel improved high-gain quadratic DC–DC converter based on two synchronous power switches and a two-winding coupled inductor." Scientific Reports (2026).

[7] Arndt, Channing, Doug Arent, Faaiqa Hartley, Bruno Merven, and Alam Hossain Mondal. "Faster than you think: Renewable energy and developing countries." Annual Review of Resource Economics 11, no. 1 (2019): 149-168.

[8] Adepoju, Webster, and Mary Sanyaolu. "Comprehensive analysis and experimental design of high-gain dc-dc boost converter topologies." arXiv preprint arXiv:2412.18329 (2024).

[9] Ejuh Che, Emmanuel, Kang Roland Abeng, Chu Donatus Iweh, George J. Tsekouras, and Armand Fopah-Lele. "The impact of integrating variable renewable energy sources into grid-connected power systems: Challenges, mitigation strategies, and prospects." Energies 18, no. 3 (2025): 689.

[10] Veerabhadra, J., and Sulake Nagaraja Rao. "Comparative assessment of high gain boost converters for renewable energy sources and electrical vehicle applications." Energy Harvesting and Systems 11, no. 1 (2024): 20220144.

[11] Sarvi, Mohammad, Reza Ebrahimnaz, and Homa Zarei Zohdi. "A New High Gain DC-DC Converter for Solar System." Journal of Solar Energy Research 9, no. 4 (2024): 2115-2124.

[12] Kumar, Madhav, Kaibalya Prasad Panda, Ritula Thakur, Gayadhar Panda, Mohammed Alruwaili, and Ahmed Emara. "A Novel High-Gain Single-Switch DC-DC Converter with Voltage-Lifting Technique and Nonlinear Gain-Compensated PI Control for EV Applications." IEEE Access (2026).

[13] Imanlou, Arash, Reza Behkam, Ali Nadermohammadi, Hamed Nafisi, Hamed Heydari-Doostabad, and Gevork B. Gharehpetian. "A new high voltage gain transformer-less step-up DC–DC converter with double duty-cycles: Design and analysis." IEEE Access 12 (2024): 103388-103404.

[14] Nagar, Vishal, Kuldeep Jayaswal, Pallavi Chaturvedi, Aditya Sharma, and D. K. Palwalia. "Design and Analysis of High Gain DC-DC Converters for PV Application." In 2023 IEEE 11th Region 10 Humanitarian Technology Conference (R10-HTC), pp. 538-543. IEEE, 2023.

[15] Bajaj, Mohit, and Amit Kumar Singh. "Grid integrated renewable DG systems: A review of power quality challenges and state-of-the-art mitigation techniques." International Journal of Energy Research 44, no. 1 (2020): 26-69.

[16] Revathi, B. Sri, and Mahalingam Prabhakar. "Non isolated high gain DC-DC converter

topologies for PV applications–A comprehensive review." Renewable and Sustainable Energy Reviews 66 (2016): 920-933.

[17] Singh, Mayank, Mukh R. Yadav, and Dheeraj Kumar Dhaked. "A review on various voltage boosting topology in DC-DC converter." Recent Advances in Electrical & Electronic Engineering (Formerly Recent Patents on Electrical & Electronic Engineering) 17, no. 6 (2024): 554-572.

[18] Bayramoğlu Dişken, Nihal, and Murat Mustafa Savrun. "High-gain multiport DC-DC converter topologies for renewable energy applications: A comprehensive review." Electric Power Components and Systems 52, no. 8 (2024): 1459-1473.

[19] Pandey, Aakriti, and Swapnajit Pattnaik. "Design and analysis of extendable switched-inductor and capacitor-divider network based high-boost DC-DC converter for solar PV application." IEEE Access 10 (2022): 66992-67007.

[20] Ruiz-Robles, Dante, Xavier Alcíbar-Martínez, Tania Sandoval-Valencia, Jesús Alejandro Franco, and Quetzalcoatl Hernandez-Escobedo. "High-Gain Bidirectional Isolated DC-DC Converter for PV-BESS Systems Using a 10 kHz Ferrite-Core Transformer: Design, Simulation, and Experimental Validation." Results in Engineering (2025): 108078.

[21] Sandoval-Valencia, Tania, Dante Ruiz-Robles, Jorge Ortíz-Marín, Jesus Alejandro Franco, Quetzalcoatl Hernandez-Escobedo, and Edgar Moreno-Goytia. "Isolated high-gain DC-DC converter with nanocrystalline-core transformer: Achieving 1: 16 voltage boost for renewable energy applications." Technologies 12, no. 12 (2024): 246.

[22] Jeyaraj, A., and K. S. Saji. "Enhanced quadratic DC-DC boost converter with integrated power factor enhancement: advancing high-voltage gain and power quality in electric vehicle charging." Electrical Engineering 107, no. 9 (2025): 11249-11271.

[23] Misal, Shrikant, and Mummadi Veerachary. "Analysis of a fourth-order step-down converter." IEEE Transactions on Industry Applications 56, no. 3 (2020): 2773-2787.

[24] Hashemzadeh, Seyed Majid, and Seyed Hossein Hosseini. "Design of a high voltage gain converter using coupled inductor with reduced voltage stress for photovoltaic energy based systems." Scientific Reports 14, no. 1 (2024): 21455.

[25] Al-Araji, Zainab Hussam, Muhanad D. Hashim Almawlawe, and Musa Hadi Wali. "Comprehensive characterization of switching and conduction losses in high-ratio step-down converters for next-generation electric vehicles." Sustainable Engineering and Innovation 7, no. 2 (2025): 449-462.